# Stress corrosion cracking behaviour of a surface-modified magnesium alloy

P. Bala Srinivasan,* C. Blawert, W. Dietzel and K.U. Kainer

*Institute of Materials Research, GKSS-Forschungszentrum Geesthacht GmbH, D21502 Geesthacht, Germany*

The effect of plasma electrolytic oxidation (PEO) treatment on the stress corrosion cracking (SCC) of a cast magnesium alloy was assessed. Even though the PEO coating has offered improved corrosion resistance, as evidenced in electrochemical tests, its effect in improving the SCC resistance in ASTM D1384 test solution was only marginal. The SCC behaviour of PEO-coated specimens was attributed to the development of microcracks in the coating, leading to cracking of the substrate under slow strain rate test conditions.

In recent times, magnesium alloys, owing to their excellent combination of properties, have found numerous applications in the electronic, automobile and aerospace industries. However, these alloys suffer heavily on account of their poor corrosion resistance in many environments [1–3] and many of the alloys have been reported to exhibit a high degree of susceptibility to environmentally assisted cracking [4–6]. A good number of surface modification procedures have been developed and used with a reasonable degree of success in different applications [7–9]. The plasma electrolytic oxidation (PEO) treatment has been found to be quite effective in improving the tribological and corrosion properties of magnesium alloys [10–12]. Even though many researchers have assessed the general corrosion behaviour of PEO-coated magnesium alloys, there seems to be no published information available on the stress corrosion cracking behaviour of magnesium alloys with a PEO coating. This work addresses the electrochemical corrosion and stress corrosion cracking behaviour of a cast magnesium alloy, with and without a silicate-based PEO coating.

Magnesium alloy specimens corresponding to the alloy designation AM50 were received in the as-cast condition. Specimens of size 30 mm × 30 mm × 5 mm were ground successively in 320, 500, 800, 1000 and 2500 grit emery sheets for the PEO treatment. The PEO treatment was carried out using a simple DC power supply source of 600 V, with 4 A capacity. The specimens were PEO-coated in an electrolyte constituted by 10 g l$^{-1}$ sodium hydroxide and 10 g l$^{-1}$ sodium silicate in double-distilled water. The PEO treatment was performed at a current density of 15 mA cm$^{-2}$, to a final voltage of 420 V. The coating process was continued at 420 V until the current reduced to close to zero, evidenced by the reduction in sparks. The temperature of the electrolyte was maintained in the range 15–25 °C and the electrolyte was stirred using a magnetic stirrer.

Electrochemical measurements were made in an ACM Gill AC potentiostat/galvanostat FRA, using a three-electrode cell. The corrosion potential of the specimens was measured for a period of 1800 s before performing the electrochemical tests. Electrochemical impedance measurements were performed with an applied amplitude of 10 mV in the frequency range 0.1–30,000 Hz at the corrosion potential. Potentiodynamic polarization studies were carried out at a sweep rate of 0.5 mV s$^{-1}$. The uncoated specimens were prepared by polishing up to 2500 grit emery for the electrochemical studies, while the PEO-coated specimens were used in the as-coated condition. Experiments were carried out in duplicate to ascertain their reproducibility, and all the experiments were performed at ambient temperature (21 ± 2 °C) in as-prepared ASTM D1384 solution containing 148 mg Na$_2$SO$_4$, 165 mg NaCl and 138 mg NaHCO$_3$ in 1 l of double-distilled water.

* Corresponding author. Tel.: +49 4152 871997; fax: +49 4152 871909; e-mail: bala.srinivasan@gkss.de

The tensile specimens for the slow strain rate tensile (SSRT) tests were of cylindrical configuration, with a 5 mm gauge diameter and 10 mm gauge length. The overall length of the specimen was 100 mm. SSRT tests were performed in ASTM D1384 test solution by following the ISO standard 7359 – Part 7 [13]. In SSRT tests in air the specimen elongation was measured using a clip-on gauge in addition to the employment of two linear variable displacement transducers (LVDT) attached to the specimen grips.

The optical micrograph of the AM50 alloy in Figure 1 reveals the coarse-grained structure of this material, characteristic of a gravity-cast condition. The near-uniform distribution of $Mg_{17}Al_{12}$ precipitates in the matrix is also evident in this micrograph. During the PEO process, the sparking and the first discharge were noticed at a voltage level of 240 V in this electrolyte. The sparking was uniform and distributed across the whole surface of the specimens treated, and the intensity of sparks was observed to increase with increasing voltage. The maximum voltage for the PEO coating was fixed as 420 V, based on prior optimization experiments to achieve a coating thickness of around 10–15 μm. Further, this voltage level was preferred for treating large-sized specimens to avoid the problems of excessive heating of the electrolyte and the consequent burning of specimens. Thickness measurements made using an eddy current probe showed an average thickness of around 12 μm, which was corroborated by the microscopic examination. The cross-section of a PEO-coated specimen is shown in Figure 2a, in which the near-uniform thickness across the section of the specimen can be seen. The morphology of the PEO-coated surface presented in Figure 2b reveals the presence of fine pores in the oxide structure formed on the surface.

The electrochemical impedance and polarization behaviour of the untreated and PEO-coated specimens are presented in Figure 3a and b, respectively. The corrosion resistance of the untreated AM50 alloy was observed to be around 4900 Ω cm². On the other hand, the PEO-coated specimen registered a resistance value of $6.3 \times 10^5$ Ω cm², showing a nearly two orders of magnitude enhancement in corrosion resistance. The corrosion potential of the PEO-coated specimen based on 30 min rest potential measurements, and also obtained from the $E_{corr}$ value, seems to be nobler than that of the untreated counterpart. The corrosion current density
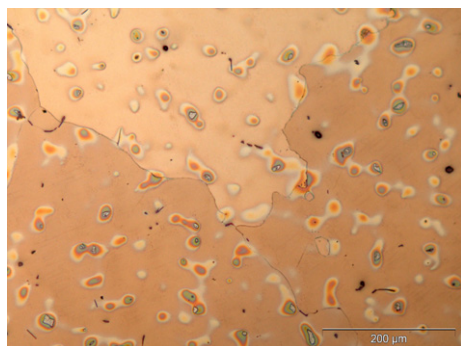


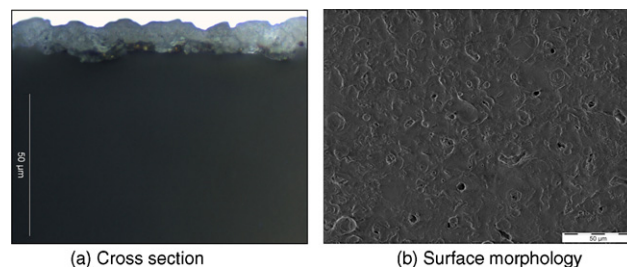(a) Cross section    (b) Surface morphology

**Figure 2.** Optical (a) and scanning electron (b) micrographs of a PEO-coated AM50 alloy.
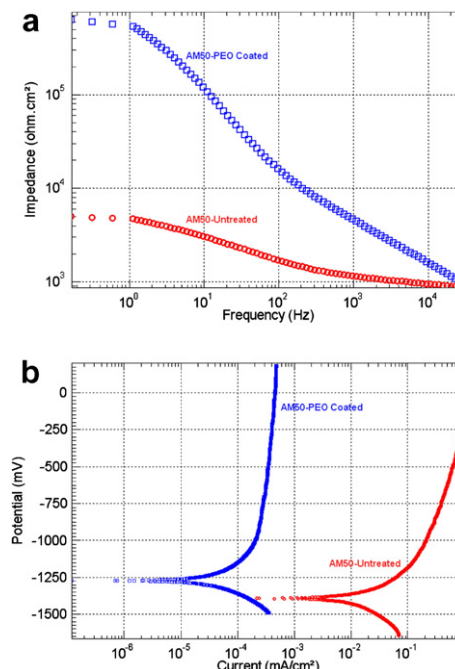


**Figure 3.** (a) Electrochemical impedance behaviour (Bode plot) of untreated and PEO-coated AM50 alloy. (b) Potentiodynamic polarization behaviour of untreated and PEO-coated AM50 alloy.

values were $1.2 \times 10^{-2}$ and $4.3 \times 10^{-5}$ mA cm$^{-2}$ for the untreated and PEO-coated specimens, respectively. The above observations, with respect to the corrosion behaviour, are in agreement with some of the documented literature [11,14,15].

The ultimate strength and the elongation values of the untreated specimen were 200 MPa and 24%, respectively, and that of the PEO-coated specimen were 185 MPa and 23%, respectively. The optical macrographs of the untreated and coated specimens subjected to tensile tests in air, shown in Figure 4a and b, suggest that the tensile deformation behaviour in these specimens might have been similar. However, there was a marginal difference in the elongation values between the specimens, which could be attributed to the presence of the brittle ceramic coating of the PEO specimen. On the other hand, the reason for the marginal lowering of the tensile strength in the PEO specimen is not known. In a work on nitrocarburizing, the development of a hard nitride/carbonitride layer was reported to lower the ultimate tensile strength of austenitic stainless steel [16]. Correlating the cited literature, it is postulated that
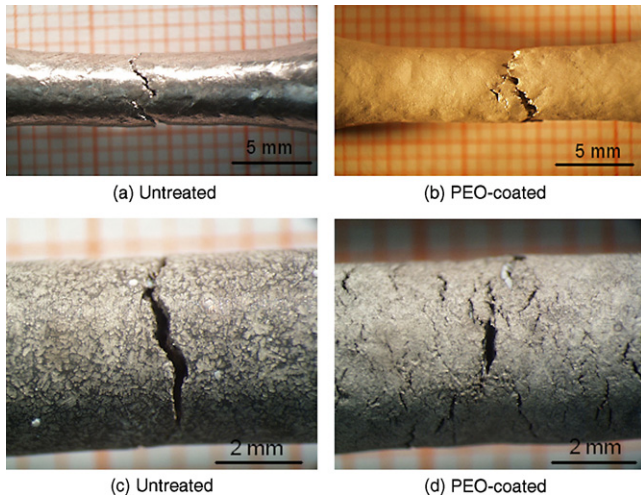


**Figure 1.** Optical micrograph of the AM50 alloy.

(a) Untreated

(b) PEO-coated



(c) Untreated

(d) PEO-coated

**Figure 4.** Optical macrographs and scanning electron micrographs showing the surface appearance of the SSRT-tested AM50 alloy in air.



(a) Untreated

(b) PEO-coated

**Figure 6.** Optical macrographs showing the surface appearance of the SSRT-tested (ASTM D1384 solution) AM50 alloy.

there could have been differences in the work-hardening behaviour during the tensile tests in the presence of the PEO coating. The higher-magnification scanning electron micrograph (Fig. 4c and d) revealed the presence of cracks in the PEO coating and also the damaged regions exposing the substrate. This suggests that the deformation characteristics were distinctly different in these two cases. This phenomenon requires further investigation.

The stress vs. strain plots of the untreated and PEO-coated specimens in air at a strain rate of 1E−6 and that of the same in ASTM D1384 test solution at a strain rate of 1E−7 are presented in Figure 5. As it was difficult to use a clip gauge in tests involving solutions, the displacement measurements were made only with LVDTs, and for uniformity and comparison purposes, the strain values measured with LVDTs are presented in this figure for all the conditions.

The untreated AM50 specimen exhibited susceptibility to stress corrosion cracking in the SSRT tests performed at $1E-7 \ s^{-1}$. The specimen failed at a stress level of around 90 MPa, with an elongation of only around 5%. Kannan et al. [17] have reported the SCC susceptibility of AZ31 wrought alloys in ASTM solutions in a recent work and Song et al. [18] documented the SCC behaviour of the same class of alloy even in
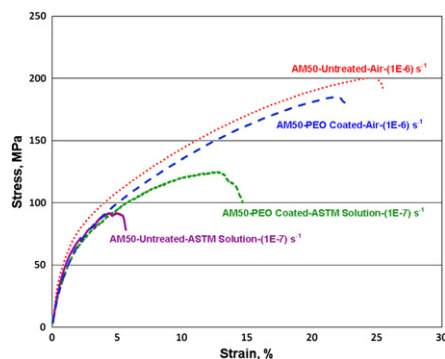
double-distilled water. Hence, it is not surprising that this cast alloy exhibited SCC in this electrolyte. The PEO-coated specimen, despite showing excellent corrosion resistance in the short-term electrochemical tests, also failed at a much lower stress level than its counterpart in air. The ultimate tensile stress value of 125 MPa is only marginally higher than that of the untreated specimen. However, the elongation was much higher, registering around 13%. The experiments were stopped as the load started to drop 20 MPa below the maximum stress values, for the assessment of the surface of the specimens. The optical macrographs of the specimens presented in Figure 6a and b give an account of the type and extent of damage on these two specimens. The untreated specimen apparently has a large crack, which would have caused the damage, while the PEO-coated specimen is observed to have developed multiple cracks. The size of the cracks that were observed in this specimen were quite large compared to those observed in the PEO-coated specimen tested in air. It is quite evident that the PEO coating, despite being thin, was cracking under conditions of constant/continuous straining, thus developing numerous microcracks. Thus, on account of the synergistic dissolution and straining at these defect sites, the cracks opened up wider and became longer, leading to SCC. The formation of numerous cracks and their widening is a plausible reason for the higher elongation values registered for the coated sample.

In summary, the PEO-coated specimen, despite showing very good resistance to corrosion in the electrochemical tests and also performing well for a relatively longer test duration (in SSRT tests), could not obviate the SCC process. It remains to be seen whether the other types of PEO coatings and/or thicker coatings of the same type would help to further palliate the SCC problems of susceptible magnesium alloys.

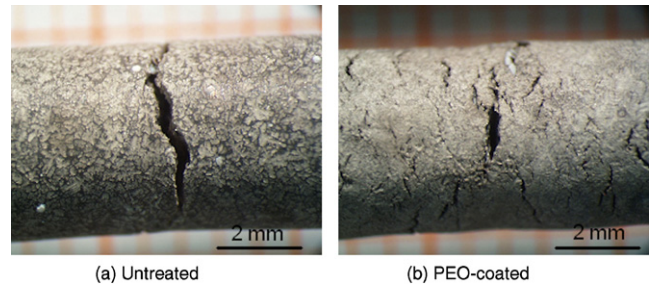**Figure 5.** Stress vs. strain plots of the untreated and PEO-coated AM50 alloy specimens in air and ASTM solution.

[1] J.E. Hillis, SAE Technical Paper No. 830523, Detroit, 1983.

[2] E. Ghali, in: R.W. Revie (Ed.), Uhlig's Corrosion Handbook, John Wiley, New York, 2000, pp. 793–830 (Chapter 44).

[3] G.L. Song, A. Atrens, Advanced Engineering Materials 1 (1999) 11–33.

[4] N. Winzer, A. Atrens, G. Song, E. Ghali, W. Dietzel, K.U. Kainer, N. Hort, C. Blawert, Advanced Engineering Materials 7 (8) (2005) 659–693.

[5] R.S. Stampella, R.P.M. Procter, V. Ashworth, Corrosion Science 24 (1984) 325.

[6] M.B. Kannan, W. Dietzel, R.K.S. Raman, P. Lyon, Scripta Materialia 57 (2007) 579–581.

[7] J.D. Gray, B. Luan, Journal of Alloys and Compounds 336 (2002) 88–113.

[8] H. Zhao, Zhanghong Huang, J. Cui, Microelectronics Engineering (2007), doi:10.1016/j.mee.2007.05.068.

[9] Z. Shi, G. Song, A. Atrens, Corrosion Science 47 (2005) 2760–2777.

[10] J. Liang, L. Hu, J. Hao, Applied Surface Science 253 (2007) 4490–4496.

[11] M. Boinet, S. Verdier, S. Maximovitch, F. Dalard, Surface and Coatings Technology 199 (2005) 141–149.

[12] C. Blawert, V. Heitmann, W. Dietzel, H.M. Nykyforchyn, M.D. Klapkiv, Surface and Coatings Technology 201 (2007) 8709–8714.

[13] International Standard ISO 7539, Corrosion of Metals and Alloys – Stress Corrosion Testing; Part 7: Slow Strain Rate Stress Corrosion Tests, International Organization for Standardization, Geneva, 1989.

[14] H. Duan, K. Du, C. Yan, F. Wang, Electrochimica Acta 51 (2006) 2898–2908.

[15] Q. Cai, L. Wang, B. Wei, Q. Liu, Surface and Coatings Technology 200 (2006) 3727–3733.

[16] P.B. Srinivasan, V. Muthupandi, S. Balaji, S. Vasudevan, N. Krishnaraj, Surface Engineering 19 (2003) 91–96.

[17] M.B. Kannan, W. Dietzel, R. Zeng, R. Zettler, J.F. dos Santos, Materials Science and Engineering A 460–461 (2007) 243–250.

[18] R.G. Song, C. Blawert, W. Dietzel, A. Atrens, Materials Science and Engineering A 399 (2005) 308–317.